

Yuanjun Liu^{1,2,3},
Yi Wang¹,
Xiang Wu¹,
Lulu Zhang²,
Jiarong Niu^{1,2,3,*}

Influence of Wave-Absorbing Functional Particles on the Electromagnetic Properties and Mechanical Properties of Coated Composites for Nickel Powders

DOI: 10.5604/01.3001.0014.2389

¹Tiangong University,
School of Textile Science and Engineering,
Tianjin 300387, China,
* e-mail: niujiarong1976@163.com

²Tianjin Municipal Key Laboratory of Advanced
Fibre and Energy Storage,
Tianjin 300387, China

³Key Laboratory of Advanced Textile Composites
of Ministry of Education,
Tianjin 300387, China

Abstract

In this subject, a single-layer coated composite for nickel powders was prepared using PU2540 polyurethane as the matrix, nickel powder as the wave-absorbing functional particle, and coating technology on plain cotton fabric. The influence of wave-absorbing functional particles on the dielectric, shielding effectiveness and mechanical properties of the single-layer coated composite for nickel powders was mainly analysed and compared. Results showed that the real and imaginary parts and loss tangent of the dielectric constant were all the largest when the iron powder was mixed with the nickel powder, and its polarizing ability, loss ability and attenuation ability with respect to electromagnetic waves were all the maximum. When the graphene was mixed with the nickel powder, the shielding attenuation ability with respect to electromagnetic waves was the best.

Key words: nickel powders, single-layer coating, electromagnetic shielding, dielectric properties.

Introduction

With the rapid development of wireless communication in the fields of industry and commerce and the military field, electronic devices tend to be more miniaturised and have higher frequency. However, the wide use of wireless devices such as mobile phones, radar and other electronic devices will cause great harm to human health, electronic instruments, and national security [1-4]. Therefore, the electromagnetic interference and electromagnetic pollution problem is paid great attention. Through study we found that shielding material and wave-absorbing material was an effective way to solve problems of electromagnetic interference

[5-9]. Electromagnetic shielding material has always followed the research idea of “thin, light, wide and strong”, as well as trying to use a variety of composite materials to meet process requirements [10-14]. Ideal electromagnetic shielding material should meet the following requirements: (1) it has ideal impedance matching, in order to attenuate the electromagnetic energy in the absorbing medium; (2) the energy formed by the electromagnetic wave incident to the material shall be converted into electrical energy, heat energy, mechanical energy and other forms of energy, so that it is attenuated in a large amount, even experiencing consumption [15-21].

In this study, a single-layer coated composite for nickel powders was prepared using PU2540 polyurethane as the matrix, nickel powder as the wave-absorbing functional particle, and coating technology on plain cotton fabric. The influence of wave-absorbing functional particles

(graphene, silver-coated copper powders, graphite, silver-coated glass beads and iron powders) (the ratio of nickel powders and wave-absorbing functional particles was 1:1) on the dielectric properties, shielding effectiveness and mechanical properties of the single-layer coated composite for nickel powders was mainly analysed and compared.

Experimental

Main experimental materials

Main experimental materials: cotton (plain woven), provided by Nantong Lin-ya Textile Co., LTD.

The main experimental drugs were shown in **Table 1**.

(1) The chemical composition of carbonyl nickel powder is as follows: nickel: 99.79%, carbon: 0.090%, oxygen: 0.11%, sulfur: 0.0010%, carbon

Table 1. Main experimental drugs.

Drug/reagent name	Specification	Manufacturer
Graphite powders	Q/HG3991-88	Tianjin Fengchuan Chemical Technology Co., LTD
Carbonyl nickel powders	W-5	Shenzhen Changxinda Shielding Materials Co., LTD
Graphene	5-15 μm	Tianjin Kairuisi Fine Chemical Co., LTD.
Silver-coated copper powders	P-30	Shenzhen Changxinda Shielding Materials Co., LTD
Silver-coated glass beads	CXD-SG3020	Shenzhen Changxinda Shielding Materials Co., LTD
Micron iron powders	1-3 μm	Shenzhen Changxinda Shielding Materials Co., LTD
Polyurethane	PU2540	Guangzhou Yuheng Environmental Protection Materials Co., LTD
Thickener	7011	Guangzhou Dianmu Composite Operating Department

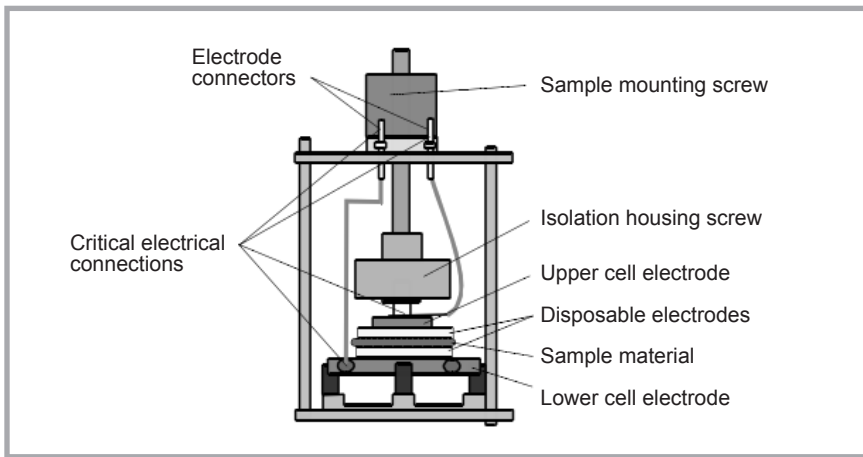


Figure 1. Test cell of the dielectric spectrometer.

monoxide: 0.001%, and iron: 0.001%; and physical properties – apparent density 0.58 g/cm³, and average particle size 2.37 μm, in the form of powder groups. The particle size distribution is D50:5 μm. (2) The chemical composition of the silver-coated hollow glass beads is as follows: Ag content 20%, and the physical properties: Scott density 1.43 g/cm³, powder resistivity 1.1 W·cm, average particle size 30 μm, distribution of particle size D10: 15 μm, D50:30 μm, and D90:35 μm, in a spherical form. (3) The properties of silver-coated copper powders are as follows: apparent density 1.6~1.8 g/cm³, reference paint resistance 0.02 W·cm, distribution of the particle size D10: ≥15.0 μm, D50:26.7~27.3 μm, and D90: ≤50 μm, with a silvery white flake appearance: PU2540 polyurethane resin has a 40% waterborne polyurethane dispersion, with excellent performance, which has the advantages of good toughness and bending resistance. The density of PU2540 polyurethane resin is 1.04 g/cm³. At 25 °C, the viscosity of PU2540 polyurethane resin is less than 300 mPa·s. The viscosity of PU2540 polyurethane resin is less than 300 mPa·s. The role of the thickener is to regulate the viscosity of polyurethane; the more

thickener there is, the greater the viscosity of polyurethane.

Preparation of materials

(1) An adequate quantity of wave-absorbing functional particles and polyurethane were taken according to the formula of the coating, leading to the mass of the absorbing agent occupying a certain proportion of that of polyurethane; and then polyurethane was mixed with additives, and stirred for 40 minutes with an electric blender. (2) After the whole absorbing agent was added into the polyurethane, the thickener was added to increase the viscosity of the coating to achieve the standard required in the experiment. The stirred coating was poured into a beaker within a suitable range, and the viscosity was measured by a viscosity meter. Finally, the preparation of the coating was finished. (3) A needle plate with a base cloth was fixed on a coating machine for small samples, adjusting parameters such as the thickness and stroke, and a coating with a certain thickness and length of 30 cm could be prepared. (4) After the coating, the coated fabric was immediately placed in a drying oven, whose temperature was maintained at 80 °C, and then dried for a certain

time. At this point, the preparation of the single-layer coating for the fabric was finished. After drying, the coating was removed and kept at room temperature until it had dried naturally.

Specific requirement of parameters of the coating

The wave-absorbing functional particle was used as the variable, and the absorbing agent of the coating (relative to the polyurethane) was selected, whose content was 10%. The viscosity was maintained at 40000 mPa·s, and the coating thickness of the nickel powders was 0.5 mm. A single-layer coated composite of five different wave-absorbing functional particles was prepared by changing the wave-absorbing functional particles.

Test indicators

Test of the dielectric constant

Tests of the real and imaginary parts of the dielectric constant and loss tangent were carried out according to GB/T 5597-1999 (Test Method of the Microwave Complex Dielectric Constant of the Solid Dielectric). The sample was correctly placed in the measuring head of a dielectric spectrometer and clamped tightly. The calculated thickness was inputted, the parameters required were then set, and finally the test was started. Figure 1 shows the test cell of the dielectric spectrometer.

Test of the shielding effectiveness

The measurement method for the shielding effectiveness of electromagnetic shielding materials is in the GB/T12190 standard. The shielding effectiveness of the coating was measured using a vector network analyser.

Test of tensile properties

According to the experimental method of GB 1447-2005 for the tensile properties of fibre-reinforced plastics, the sample size was 5 cm × 20 cm and the clamping distance 10 cm.

Table 2. Process parameters of nickel powders combining with different wave-absorbing functional particles.

Number	Wave-absorbing functional particles and its proportion	Percentage relative to polyurethane, %	Stirring time, min	Viscosity, mPa s	Coating thickness, mm	Velocity of the coating machine, cm/min	Temperature of the drying oven, °C	Drying time, min
1	Graphene: nickel powders = 1:1	10	40	40000	0.5	60	80	10
2	Silver-coated copper powders: nickel powder = 1:1	10	40	40000	0.5	60	80	10
3	Graphite: nickel powders = 1:1	10	40	40000	0.5	60	80	10
4	Silver-coated glass beads: nickel powders = 1:1	10	40	40000	0.5	60	80	10
5	Iron powders: nickel powders = 1:1	10	40	40000	0.5	60	80	10

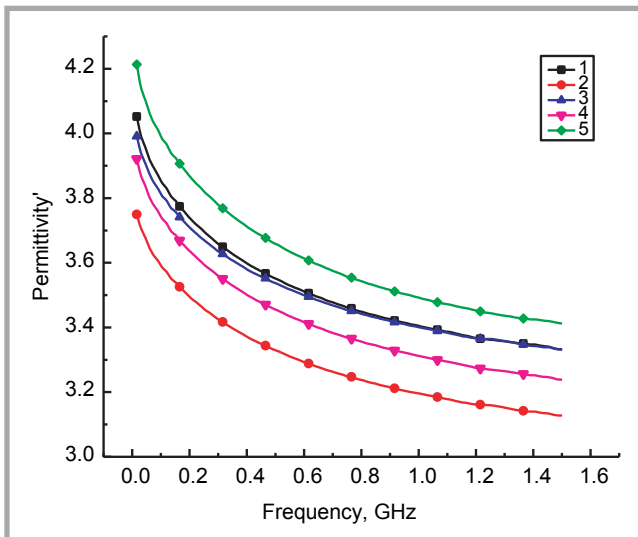


Figure 2. Influence of wave-absorbing functional particles on the real part of dielectric constant of single-layer coated composites.

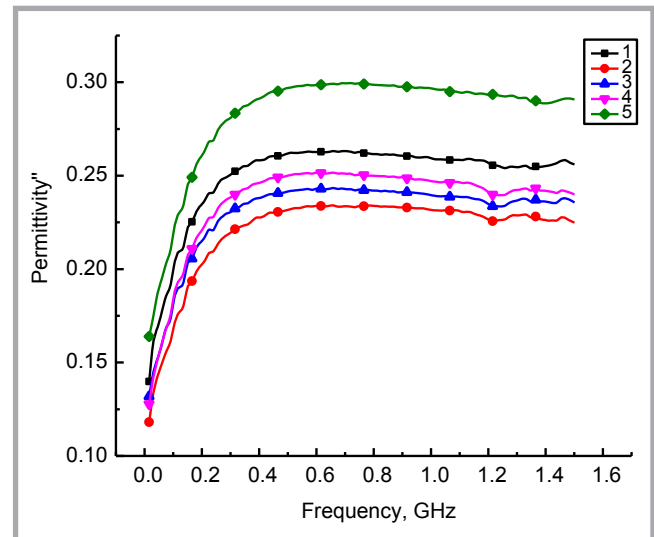


Figure 3. Influence of wave-absorbing functional particles on the imaginary part of dielectric constant of single-layer coated composites.

■ Results and discussion

Influence of wave-absorbing functional particles on the dielectric properties of single-layer coated composites

In order to study the influence of wave-absorbing functional particles on the dielectric properties (real and imaginary parts and loss tangent value) of single-layer coated composites, single-layer coated composites of five different types of wave-absorbing functional particles were prepared by changing the combination of wave-absorbing functional particles (graphene powders, silver-coated copper powders, graphite, silver-coated glass beads and iron powders) with nickel powders on plain cotton fabric. The specific process parameter is shown in **Table 2**.

The percentage relative to polyurethane referred to the total mass percentage of two types of wave-absorbing functional particles occupied for the polyurethane.

Samples of the coated fabric were prepared and the dielectric properties tested within a range from 10 MHz to 1.5 GHz. Curves of the real and imaginary parts and the loss tangent value of the dielectric constant are shown in **Figures 1, 2 and 3**, respectively.

The dielectric constant can indirectly evaluate the electromagnetic properties of microwave absorbing materials. The dielectric constant was composed of three parts: the real and imaginary parts

and the loss tangent value. The real part showed the polarisation degree of the materials under an applied electric field, where the larger the value of the real part, the greater the polarisation ability of the materials. The imaginary part showed the loss ability of the materials under an applied electric field. The larger the value of the imaginary part, which showed the re-alignment of the electric dipole moment under an applied electric field, the greater the loss ability respect to electromagnetic waves [18-19]. The loss tangent value can also indirectly show the absorption ability of materials, which was used for characterising the absorption and attenuation ability of the materials, where the larger the value thereof, the greater the attenuation ability [22-26].

As can be seen from **Figure 2**, within the range of 0.01 to 0.3 GHz, the real part of the dielectric constant for sample 5# decreased the fastest, followed by 1#, 4#, 2# and 3#. Within the range of 0.3 to 1.5 GHz, the real part of the dielectric constant for the five samples continued to decrease, among which the real part of the dielectric constant for sample 5# decreased the fastest, followed by 4#, 1#, 3# and 2#. Within the range of 0.01 to 1.5 GHz, with increasing frequencies of the applied electric field, the real part of the dielectric constant for the five samples: 1#, 2#, 3#, 4# and 5# all gradually decreased, as with the polarising ability; thus, we can know that this type of single-layer coated composite was suitable for absorbing electromagnetic waves at a low frequency. When the frequency

was 0.01 GHz, values of the real part of the dielectric constant of each sample were all at the maximum, and the polarising ability of the magnetic field produced in the coating with respect to the applied magnetic field was the strongest. Within the range of 0.01 to 1.5 GHz, with increasing frequencies of the applied electric field, the real part of the dielectric constant was the largest for sample 5#, whose polarising ability with regard to electromagnetic waves was the strongest, followed by 1#, 3#, 4# and 2#. Namely, within the range of 0.01 to 1.5 GHz, the real part of the dielectric constant of the coating of iron powders mixed with nickel powders at the given ratio was the largest, whose polarising ability was the strongest, followed by the coatings with the addition of graphene powders, graphite powders, silver-coated glass bead powders and silver-coated copper powders. The coating of nickel powders mixed with iron powders at the given ratio had the maximum value of the real part of the dielectric constant, and the strongest polarising ability.

As can be seen from **Figure 3**, within the range of 0.01 to 0.3 GHz, the imaginary part of the dielectric constant for sample 3# increased the fastest, followed by 5#, 4#(1#) and 3#. Within the range of 0.3 to 0.7 GHz, values of the imaginary part of the dielectric constant for the five samples: 1#, 2#, 3#, 4# and 5# all increased gradually. Within the range of 0.7 to 1.5 GHz, with increasing frequencies of the applied electric field, the imaginary part of the dielectric constant

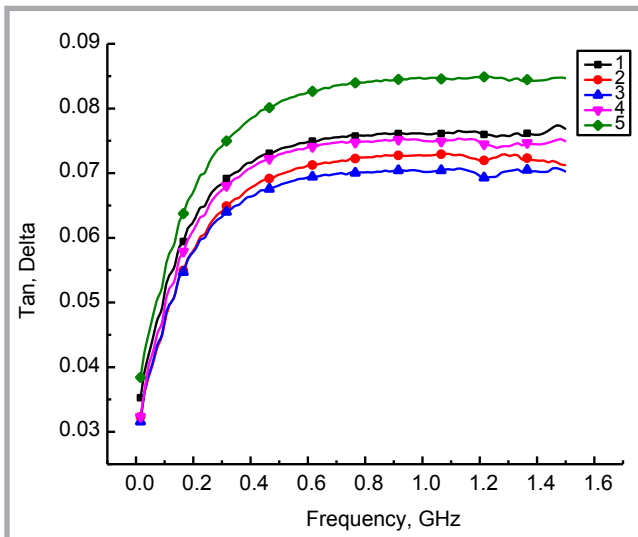


Figure 4. Influence of wave-absorbing functional particles on the tangent value loss of single-layer coated composites.

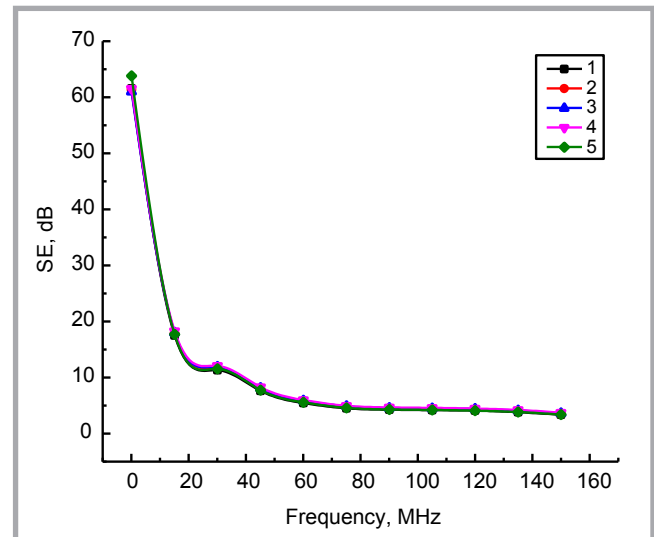


Figure 5. Influence of wave-absorbing functional particles on the shielding effectiveness of single-layer coated composites.

for the five samples – 1#, 2#, 3#, 4# and 5# all remained unchanged at first, and then had a modest decline. Within the range of 0.01 to 0.3 GHz, the imaginary part of the dielectric constant for sample 3# increased the fastest, followed by 5#, 4#(1#) and 3#. Within the range of 0.01 to 0.3 GHz, the imaginary part of the dielectric constant for the five samples: 1#, 2#, 3#, 4# and 5# all increased gradually. Within the range of 0.7 to 1.5 GHz, with increasing electric field frequencies, the imaginary part of the dielectric constant for the five samples i.e. 1#, 2#, 3#, 4# and 5# all remained unchanged at first, and then had a modest decline. Within the range of 0.01 to 1.5 GHz, with increasing frequencies of the applied electric field, the imaginary part of the dielectric constant for the five samples: 1#, 2#, 3#, 4# and 5# all increased gradually, the loss ability to electromagnetic waves also improved gradually. When the frequency was 0.01 GHz, values of the imaginary part of the dielectric constant were all at the minimum for each sample, and the loss ability with respect to electromagnetic waves was the weakest. Within the range of 0.01 to 1.5 GHz, with increasing frequencies of the applied electric field, the imaginary part of the dielectric constant for sample 5# was the largest, and the loss ability with regard to electromagnetic waves was the strongest, followed by 1#, 4#, 3# and 2#. Namely, within the range of 0.01 to 1.5 GHz, the imaginary part of the dielectric constant of the coating when iron powders were mixed with nickel powders at the given ratio was the largest, and the loss ability was the strongest, followed by

the coating containing graphene powders, silver-coated glass beads powders, graphite powders and silver-coated copper powders.. Within the range of 0.01 to 1.5 GHz, with increasing frequencies of the applied electric field, the imaginary part of the dielectric constant for the five samples: 1#, 2#, 3#, 4# and 5# all showed a trend of increasing at first and then experiencing a modest decline; the loss ability with respect to electromagnetic waves also showed a trend of increasing at first and then experiencing a modest decline. When the frequency of the applied electric field was 0.5 GHz, the value of the imaginary part reached the maximum value, and the loss ability of the magnetic field produced in the coating with respect to the applied magnetic field was the strongest. The imaginary part of the dielectric constant of the coating when iron powders were mixed with nickel powder at the given ratio was the largest, and the loss ability was the strongest.

As can be seen from **Figure 4**, within the range of 0.01 GHz to 0.7 GHz, the increased speed of the loss tangent value for the five samples: 1#, 2#, 3#, 4# and 5# was almost the same. Within the range of 0.7 to 1.5 GHz, with increasing frequencies of the applied electric field, the loss tangent value of 5# had a modest increase, while that of 1#, 2#, 3# and 4# remained the maximum. Within the range of 0.01 to 1.5 GHz, with increasing frequencies of the applied electric field, loss tangent values for the five samples – 1#, 2#, 3#, 4# and 5# all increased gradually, and the attenuation ability with regard to

electromagnetic waves also rose gradually. When the frequency was 0.01 GHz, the loss tangent values of each sample were at the minimum, and the attenuation ability with respect to electromagnetic waves was the weakest. Within the range of 0.01 to 1.5 GHz, with increasing frequencies of the applied electric field, the loss tangent value of 5# was at the maximum, and the attenuation ability of electromagnetic waves was the strongest, followed by 1#, 4#, 2# and 3#. Within the range of 0.01 to 1.5 GHz, the loss tangent value of the coating when iron powders were mixed with nickel powders at the given ratio was the largest, and the attenuation ability was the strongest, followed by the coating containing graphene powders, silver-coated glass beads powders, silver-coated copper powders and graphite powders. Within the range of 0.01 to 1.5 GHz, with increasing frequencies of the applied electric field, the loss tangent value of the five samples: 1#, 2#, 3#, 4# and 5# all remained unchanged after first increasing. When the frequency of the applied electric field was 0.8 GHz, the loss tangent value reached the maximum, and the attenuation ability of the magnetic field produced in the coating with respect to the applied magnetic field was the strongest.

Influence of wave-absorbing functional particles on the shielding effectiveness of single-layer coated composites

In order to study the influence of wave-absorbing functional particles on the shielding effectiveness of single-layer coated composites, single-layer coat-

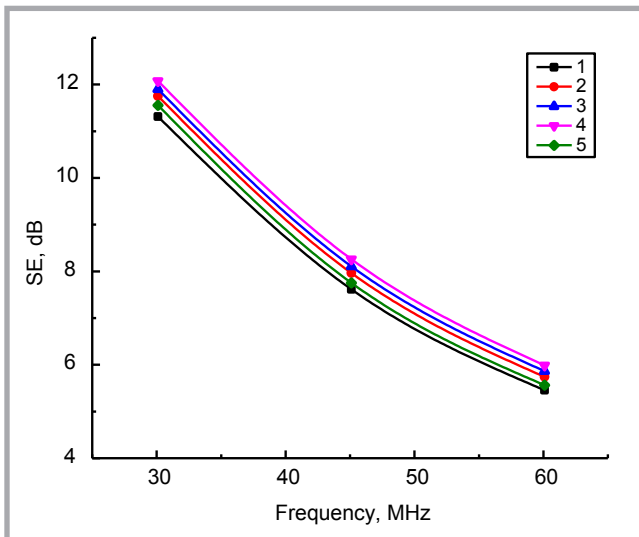


Figure 6. Influence of wave-absorbing functional particles on the shielding effectiveness of single-layer coated composites.

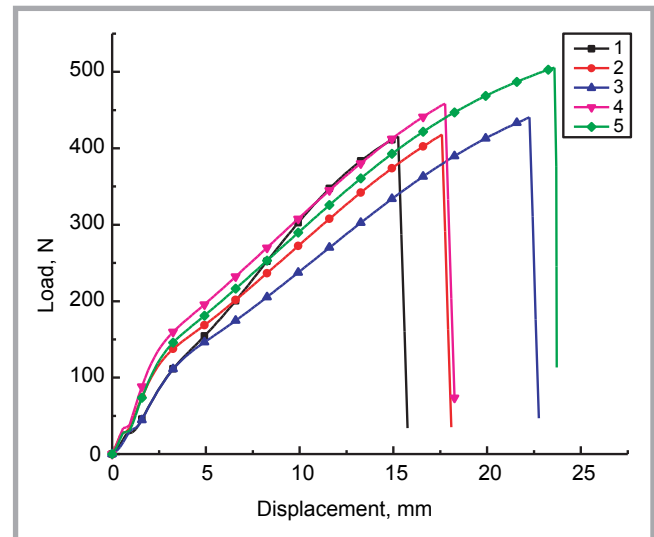


Figure 7. Influence of wave-absorbing functional particles on the tensile strength of single-layer coated composites.

ed composites of five different types of wave-absorbing functional particles were prepared by changing the combination of wave-absorbing functional particles (graphene powders, silver-coated copper powders, graphite, silver-coated glass beads and iron powders) with nickel powders on plain cotton fabric. The specific process parameter is shown in **Table 2**.

Samples of coated fabric were prepared, the t shielding attenuation value was tested in a test range of 100 kHz to 1.5 GHz. The curve of the frequency-shielding attenuation value is shown in **Figures 5 and 6** (amplification of **Figure 5**).

Table 1 shows that the resistivity of graphene was 10^{-6} W·cm, the resistivity of silver-coated copper powders $0.02 \Omega\cdot\text{cm}$, that of graphite $(8\text{--}13)\times 10^{-4} \Omega\cdot\text{cm}$, that of silver-coated glass beads $1.1 \Omega\cdot\text{cm}$, that of iron powders $9.78\times 10^{-6} \Omega\cdot\text{cm}$, and that of nickel powders was $6.9\times 10^{-6} \Omega\cdot\text{cm}$. Thus it was concluded that the order of resistivity of wave-absorbing functional particles was graphene < nickel powders < iron powders < graphite < silver-coated copper powders < silver-coated glass beads, and the order of conductive properties of wave-absorbing functional particles was graphene > nickel powders > iron powders > graphite > silver-coated copper powders > silver-coated glass beads. Free electrons in graphene were really free, which were almost not limited by carbon atoms; thus, the resistivity was very small, as well as the resistance, and the electric conductivity was the best,

which was more than that of all metal. The shielding effectiveness was related to the electric conductivity, the better the conductivity of the coating, the better the shielding effectiveness [33].

As can be seen in **Figure 5**: within the range of 0.1 MHz to 150 MHz, with increasing frequencies of the applied electric field, the shielding attenuation values of the five samples – 1#, 2#, 3#, 4# and 5# all gradually decreased, with the decreasing speed being about the same. Within the range of 60 to 150 MHz, with increasing frequencies of the applied electric field, the shielding effectiveness of the five samples continued to decrease, but the decreasing speed had obviously decreased. Within the range of 0.1 to 150 MHz, with increasing frequencies of the applied electric field, the shielding attenuation values of the five samples – 1#, 2#, 3#, 4# and 5# all gradually decreased, and the shielding effect with respect to electromagnetic waves fell; thus, when the frequency was 0.1 MHz, the largest shielding attenuation value was obtained. When the frequency was 0.1 MHz, the maximum values of the shielding atten-

uation of 1 #, 2 #, 3 #, 4 # and 5 # were 61.56 dB, 61.37 dB, 61.00 dB, 61.51 dB and 63.80 dB, respectively. As can be seen from **Figure 6**, within the range of 30 to 60 MHz, with increasing frequencies of the applied electric field, the shielding attenuation value of 1# was the strongest, as well as the shielding attenuation ability with regard to electromagnetic waves, followed by 5#, 2#, 3# and 4#. Within the range of 0.1 to 150 MHz, with increasing frequencies of the applied electric field, the shielding attenuation value of the coating whose added functional particles were silver-coated glass beads remained the largest, the shielding attenuation ability the strongest, and the shielding effectiveness was the best, followed by the coatings with the addition of graphite powders, silver-coated copper powders, iron powders and graphene powders. The shielding attenuation value decreased in turn, and the shielding attenuation with respect to electromagnetic waves also decreased. Within the range of 0.1 to 150 MHz, with increasing frequencies of the applied electric field, the order of shielding effectiveness of the coating with the addition of functional

Table 3. Parameters of the mechanical properties of different wave-absorbing functional particles.

Number	The maximum load, N	The maximum load-displacement, mm	The tensile stress value of the maximum load, MPa	The elasticity modulus, MPa
1	385.7225	15.42316	7.71445	105.24088
2	364.33765	16.42323	7.28675	86.93659
3	507.21219	21.59006	10.14424	94.89884
4	394.11127	11.92333	7.88223	102.56672
5	444.32272	19.75661	8.88645	90.87496

particles was silver-coated glass beads > graphite > silver-coated copper powders > iron powders > graphene.

Influence of wave-absorbing functional particles on the mechanical properties of single-layer coated composites

In order to study the influence of wave-absorbing functional particles on the mechanical properties of single-layer coated composites, single-layer coated composites of five different types of wave-absorbing functional particles were prepared by changing the combination of wave-absorbing functional particles (graphene powders, silver-coated copper powders, graphite, silver-coated glass beads and iron powders) with nickel powders on plain cotton fabric. The specific process parameter is shown in **Table 2**.

A test of the tensile properties of the materials was carried out on an Instron universal material experiment machine. The parameter of the mechanical properties is shown in **Table 3**.

Samples of the coated fabric were prepared. The curve of the displacement-load is shown in **Figure 7**.

It can be seen from **Figure 7** that when $0 < d < 5$ mm (d was the displacement), the displacement-load curves of 1#, 2#, 3#, 4# and 5# showed a nonlinear change, while when $5 < d < 30$ mm, with increasing displacements and loads increasing gradually, the curves of each sample started to show a linear change until the samples experienced rupture. When the load reached the maximum (that is, the maximum load-displacement value), the coated fabric began to experience rupture, while with increasing displacements, the load decreased. When $0 < d < 25$ mm, with increasing displacements, 4# reached the maximum load first, the value of that of 1#, 5# and 3#. The maximum load of 3 # was the largest, followed by 5#, 4#, 1#, and 2#.

Conclusions

1. Within the range of 0.01 to 1.5 GHz, the real part of the dielectric constant of the coating of iron powders mixed with nickel powders at the given ratio was the largest, and the polarising ability was the strongest, followed by coatings with the addition of

graphene powders, graphite powders, silver-coated glass bead powders and silver-coated copper powders. When the frequency was 0.01 GHz, values of the real part of the dielectric constant of each sample were all at the maximum, and the polarising ability of the magnetic field produced in the coating with respect to the applied magnetic field was the strongest.

2. Within the range of 0.01 to 1.5 GHz, the imaginary part of the dielectric constant of the coating when iron powders were mixed with nickel powders at the given ratio was the largest, and the loss ability was the strongest followed by coatings containing graphene powders, silver-coated glass bead powders, graphite powders and silver-coated copper powders. When the frequency of the applied electric field was 0.5 GHz, the value of the imaginary part reached the maximum value, and the loss ability of the magnetic field produced in the coating with respect to the applied magnetic field was the strongest.
3. Within the range of 0.01 to 1.5 GHz, the loss tangent value of the coating when iron powders were mixed with nickel powders at the given ratio was the largest, and the attenuation ability was the strongest, followed by coatings containing graphene powders, silver-coated glass bead powders, silver-coated copper powders and graphite powders. When the frequency of the applied electric field was 0.8 GHz, the loss tangent value reached the maximum, and the attenuation ability of the magnetic field produced in the coating with respect to the applied magnetic field was the strongest.
4. Within the range of 0.1 to 150 MHz, with increasing frequencies of the applied electric field, the shielding attenuation value of the coating with added functional particles of silver-coated glass beads remained the largest, the shielding attenuation ability the strongest, and the shielding effectiveness was the best, followed by coatings with the addition of graphite powders, silver-coated copper powders, iron powders and graphene powders, with the shielding attenuation value decreasing in turn. When the frequency was 0.1 MHz, the largest shielding attenuation value of each sample was obtained.

Acknowledgements

The authors would like to acknowledge Project No. 2019M661030, 2019TQ0181, 18JCZDJC99900, TJPU2K20170105, 2017 KJ070, and Project No.201710058074. Special acknowledgement goes to the project funded by the China Postdoctoral Science Foundation.

References

1. Liu YJ, Liu YC, Zhao XM. The Research of EM Wave Absorbing Properties of Ferrite/Silicon Carbide Double Coated Polyester Woven Fabric. *Journal of the Textile Institute*, 2018; 109: 106-112.
2. Li HC, Qian XR, Li TL, Ni YH. Percolation for Coated Conductive Paper: Electrical Conductivity as a Function of Volume Fraction of Graphite and Carbon Black. *Bioresources* 2015; 10: 4877-4885.
3. Liu YJ, Liu BC, Zhao XM. The Influence of the Type and Concentration of Oxidants on the Dielectric Constant of the Polypyrrole-Coated Plain Woven Cotton Fabric. *Journal of the Textile Institute* 2018; 109(9): 1127-1132.
4. Sobha AP, Narayanankutty SK. Improved Strain Sensing Property of Functionalised Multiwalled Carbon Nanotube/ Polyaniline Composites in TPU Matrix. *Sensors and Actuators A-physical* 2015; 233: 98-107.
5. Li J, Bi S, Mei B, Shi F, Cheng WI, Su XJ, Wang J J. Effects of Three-Dimensional Reduced Graphene Oxide Coupled with Nickel Nanoparticles on the Microwave Absorption of Carbon Fiberbased Composites. *Journal of Alloys and Compounds* 2017; 717: 205-213.
6. Liu YJ, Zhao XM, Tuo X. Study of Graphite/Silicon Carbide Coating of Plain Woven Fabric for Electrical Megawatt Absorbing Properties. *Journal of the Textile Institute* 2017; 108(4): 483-488.
7. Ren F, Song DP, Li Z, Jia LC, Zhao YC, Yan DX, Ren PG. Synergistic Effect of Graphene Nanosheets and Carbonyl Iron-Nickel Alloy Hybrid Filler on Electromagnetic Interference Shielding and Thermal Conductivity of Cyanate Ester Composites. *Journal of Materials Chemistry C* 2018; 6: 1476-1486.
8. Sambal P, Dhawan SK, Gairola P, Chauhan SS, Gairola SP. Synergistic Effect of Polypyrrole/BST/RGO/Fe₃O₄ Composite for Enhanced Microwave Absorption and EMI Shielding in X-Band. *Current Applied Physics* 2018; 18: 611-618.
9. Lin SF, Ju S, Zhang JW, Shi G, He YL, Jiang DZ. Ultrathin Flexible Graphene Films with High Thermal Conductivity and Excellent EMI Shielding Performance Using Large-Sized Graphene Oxide Flakes. *Rsc Advances* 2019; 9: 1419-1427.
10. Nazir A, Yu HJ, Wang L, Haroon M, Ullah RS, Fahad S, Usman M. Recent Progress in the Modification of Carbon Materials and their Application in Com-

- posites for Electromagnetic Interference Shielding. *Journal of Materials Science* 2018; 53: 8699-8719.
11. Xiang C, Guo RH, Lin SJ, Jiang SX, Lan JW, Wang C, Zhang Y. Lightweight and Ultrathin $\text{TiO}_2\text{-Ti}_3\text{C}_2\text{TX/Graphene}$ Film with Electromagnetic Interference Shielding. *Chemical Engineering Journal* 2019; 360: 1158-1166.
 12. Li Y, Sun L, Xu F, Wang SS, Peng QY, Yang ZY, Li YB. Electromagnetic and acoustic double-shielding graphene-based metastructures. *Nanoscale* 2019; 11: 1692-1699.
 13. Yuan HR, Zhang X, Yan F, Zhang S, Zhu CL, Li CY, Chen YJ. Nitrogen-Doped Carbon Nanosheets Containing Fe_3C Nanoparticles Encapsulated in Nitrogen-Doped Graphene Shells for High-Performance Electromagnetic Wave Absorbing Materials. *Carbon*, 2018; 140: 368-376.
 14. Zhu HX, Yang YQ, Duan HJ, Zhao GZ, Liu YQ. Electromagnetic Interference Shielding Polymer Composites with Magnetic and Conductive Feco/Reduced Graphene Oxide 3D Networks. *Journal of Materials Science-materials in Electronics* 2019; 30: 2045-2056.
 15. Liu YJ, Liu YC, Zhao XM. The Research of EM Wave Absorbing Properties of Ferrite/Silicon Carbide/Graphite Three-Layer Composite Coating Knitted Fabrics. *Journal of the Textile Institute* 2016; 107: 483-492.
 16. Li BZ, Weng XD, Sun XD, Zhang Y, Lv XL, Gu GX. Facile Synthesis of Fe_3O_4 /Reduced Graphene Oxide/Polyvinyl Pyrrolidone Ternary Composites and Their Enhanced Microwave Absorbing Properties. *Journal of Saudi Chemical Society* 2018, 22: 979-984.
 17. Quan L, Qin FX, Estevez D, Wang H, Peng HX. Magnetic Graphene for Microwave Absorbing Application: Towards the Lightest Graphene-Based Absorber. *Carbon* 2017; 125: 630-639.
 18. Li Z, Haigh A, Soutis C, Gibson A. X-Band Microwave Characterisation and Analysis of Carbon Fibre-Reinforced Polymer Composites. *Composite Structures* 2019; 208: 224-232.
 19. Liu YJ, Liu YC, Zhao XM. The Influence of Dopant on the Dielectric Properties of Flexible Polypyrrole Composites. *Journal of the Textile Institute* 2017; 108: 1280-1284.
 20. Li Q, Yin XW, Duan WY, Cheng LF, Zhang LT. Improved Dielectric Properties of PDCS-Sicn by In-Situ Fabricated Nano-Structured Carbons. *Journal of the European Ceramic Society* 2017; 37: 1243-1251.
 21. Barannik AA, Cherpak NT, Protsenko IA, Gubin AI, Kieev D, Vitusevich S. Contactless Exploration of Graphene Properties Using Millimeter Wave Response of WGM Resonator. *Applied Physics Letters* 2018; 113: 094102.
 22. Liu Y, Zhao X. Experimental Studies on the Dielectric Behaviour of Polyester Woven Fabrics. *FIBRES & TEXTILES in Eastern Europe* 2016; 24, 3(117): 67-71. DOI: 10.5604/12303666.1196614.
 23. Gao X, Wang Y, Wang Q G, Wu X M, Zhang W Z, Zong M, Zhang L J. Facile Synthesis Of A Novel Flower-Like BiFeO_3 Microspheres/Graphene with Superior Electromagnetic Wave Absorption Performances. *Ceramics International* 2019; 45: 3325-3332.
 24. Liu YJ, Zhao XM, Tuo X. Preparation of Polypyrrole Coated Cotton Conductive Fabrics. *Journal of the Textile Institute* 2017; 108(5): 829-834.
 25. Liu YJ, Liu YC, Zhao XM. The Influence of Pyrrole Concentration on the Dielectric Properties of Polypyrrole Composite Material. *The Journal of the Textile Institute*, 2017; 108(7): 1246-1249.
 26. Liu YJ, Zhao XM, Tuo X. The Research of EM Wave Absorbing Properties of Ferrite/Silicon Carbide/Graphite Three-Layer Composite Coating Knitted Fabrics. *Journal of the Textile Institute* 2016; 107(4): 483-492.

Received 14.05.2019 Reviewed 06.03.2020



The 2020 Virtual Textile Sustainability Conference offers an unparalleled opportunity to



EXPLORE
emerging trends and opportunities in sustainability



CONNECT
with a diverse group of change-makers from around the globe



LEARN
from experts on today's most pressing sustainability topics



[Contact us](mailto:Conference@TextileExchange.org)
Conference@TextileExchange.org